1146 *J. Am. Chem. Soc.* **1986**, *108*, 1146-1149

Resolution and Characterization of Rotamers in 1-Phenyl-2-(2-anthryl)ethylene

K. P. Ghiggino,[*][†] P. F. Skilton,[†] and E. Fischer[‡]

Contribution from the Department of Physical Chemistry, University of Melbourne, Victoria, Australia 3052, and the Department of Structural Chemistry, The Weizmann Institute of Science, Rehovot 76100, Israel. *Received August 6, 1985*

Abstract: Time-resolved spectroscopic techniques have enabled the components of the heterogeneous fluorescence of 1-phenyl-2-(2-anthryl)ethylene to be resolved in toluene solution. The emission is rationalized in terms of two species with lifetimes and quantum yields at 25 °C measured to be $\tau_1 = 8.3$ ns and $\phi_1 = 0.24$ and $\tau_2 = 28.25$ ns and $\phi_2 = 0.97$, each with its own distinctive fluorescence and absorption spectra. It is shown that the difference in fluorescence decay times of these two rotameric species is attributable to a difference in their nonradiative rates. Temperature dependence measurements of fluorescence decay have enabled the enthalpy of the equilibrium in the ground state to be estimated at 4.5 kJ/mol with the shorter lived, more Stokes-shifted species favored at higher temperatures.

In recent years, considerable evidence has been acquired supporting the existence of ground-state rotamers in solutions of trans aryl ethylenes.[1-9] Some workers have observed either dual exponential decays of fluorescence[6,10] or excitation wavelength dependence of emission profiles[1,9,10] and quantum yields,[4,11] with these photophysical properties being independent of rigorous purifications.[2,4,6] Indeed the apparent number of emitting species has been correlated with conformeric forms being present in solution due to rotation about the aryl–ethylene single bond.[9] Calculations[12,13] have supported this view by demonstrating the presence of more than one energetically favorable configuration, with the different rotamers being nearly isoenergetic yet separated by a significant barrier to rotation. Recently, studies with model compounds for 1-phenyl-2-(2-naphthyl)ethylene,[3] where the molecule is either bridged or sterically hindered so that it adopts these postulated configurations, have indicated that different emission spectra can be attributed to these rotamers and that the more red-shifted fluorescence is associated[3,11] with the more sterically crowded form.

In most studies, resolution of component fluorescent emissions from the aryl ethylenes has been performed qualitatively by observing spectral variations while exciting at different wavelengths.[9,12] This procedure has suggested that 1-phenyl-2-(2-anthryl)ethylene (Ph-2A, Figure 1) and related compounds have an emission composed of two contributions, one being at lower energies than the other. By analogy to Saltiel and Eaker[3] this lower energy species should have a structure similar to b. In Ph-2A there is a particularly marked difference[9] in the fluorescence spectra of the two rotameric forms. For this reason, time-resolved spectroscopy both in the temporal and spectral domains has now been employed not only to definitively resolve these component emissions but also to characterize each with its own decay lifetime and quantum yield. In addition, the high resolution absorption spectra have been calculated for each rotamer. The analysis has allowed the determination of the rates for the radiative and non-radiative relaxation processes for each rotamer and the estimation of the energy difference between the ground-state species.

Experimental Section

The sample of Ph-2A was kindly donated by Professor A. E. Siegrist. Its preparation and purification have been described elsewhere.[9,14] Toluene (AR grade, May and Baker) was purified[15] by repeated shaking with H_2SO_4 (AR grade, May and Baker) until all traces of cloudiness were gone, followed by fractional distillation and storage under nitrogen. The purified toluene was observed to be free of all fluorescent impurities in the spectral regions of interest. This solvent was chosen due to the relative insolubility of Ph-2A in other solvent systems. All solutions were prepared to have a maximum optical density of less than 0.5 at the excitation wavelength and were thoroughly degassed by repeated freeze–pump–thaw cycles, the exception being the absorption experiments where the samples were undegassed. Quartz rectangular cells were used throughout. Unless specified otherwise, all fluorescence and absorption measurements were thermostated at 25.0 °C using a Bruan Thermomix 1420.

Absorption spectra relative to a solvent reference at 25 °C were recorded and digitized at 0.8-nm intervals on an Hitachi 150-20 spectrophotometer. Steady-state emission and excitation spectra were recorded on a Perkin-Elmer MPF-44A fluorescence spectrometer by using a 2-nm bandpass. Quantum yields were obtained relative to a β-carboline fluorescence standard[16] ($\phi_{BC} = 0.60$) by using corrected emission spectra[16] and employing eq 1 with solutions of similar absorbances so as to minimize geometrical considerations. *A* is the absorbance at the

$$\phi_U = \phi_{BC}\left(\frac{n_U}{n_{BC}}\right)^2\left(\frac{I_U}{I_{BC}}\right)\left(\frac{1 - 10^{-A_{BC}}}{1 - 10^{-A_U}}\right) \qquad (1)$$

wavelength of excitation, *n* is the refractive index, *I* is the integrated intensity $\int I(\bar{\nu})\, d\bar{\nu}$ of the corrected fluorescence spectrum, and the subscripts U and BC refer to the unknown and β-carboline samples, respectively. Fluorescence decay curves were recorded by time-correlated single-photon counting by using as an excitation source a mode-locked Ar^+ ion laser synchronously pumping a cavity-dumped Rhodamine 6G dye laser (Spectra Physics). The output of the dye laser was frequency doubled by using a temperature-tuned ADA crystal providing vertically polarized light pulses at 295 nm with a 4-MHz repetition rate. Emission from the sample was passed through a polarizer set at 54.7° to the excitation polarization and focused onto the slits of a Jobin-Yvon H-20 holographic grating monochromator before being detected by a Philips XP 2020Q photomultiplier tube. The time-correlated single-photon-

---

[†] University of Melbourne.

[‡] The Weizmann Institute of Science

(1) Fischer, G.; Fischer, E. *J. Chem. Soc., Perkin Trans. 2* **1981**, 1264.

(2) Wismontski-Knittel, T.; Das, P. K.; Fischer, E. *J. Phys. Chem.* **1984**, *88*, 1163.

(3) Saltiel, J.; Eaker, D. W. *J. Am. Chem. Soc.* **1984**, *106*, 7624.

(4) Birks, J. B.; Bartocci, G.; Aloisi, G. G.; Dellonte, S.; Barrgelletti, F. *Chem. Phys.* **1980**, *51*, 113.

(5) Alfimov, M. V.; Razumov, V. F.; Rachinsky, A. G.; Listvan, V. N.; Scheck, Y. B. *Chem. Phys. Lett.* **1983**, *101*, 593.

(6) Haas, E.; Fischer, G.; Fischer, E. *J. Phys. Chem.* **1978**, *82*, 1638.

(7) Fischer, E. *J. Photochem.* **1985**, *28*, 139.

(8) Alfimov, M. V.; Scheck, Y. B.; Kovalenko, N. P. *Chem. Phys. Lett.* **1976**, *43*, 154.

(9) Fischer, G.; Fischer, E. *J. Phys. Chem.* **1981**, *85*, 2611.

(10) Ghiggino, K. P. *J. Photochem.* **1980**, *12*, 173.

(11) Fischer, G.; Seger, G.; Muszkat, K. A.; Fischer, E. *J. Chem. Soc., Perkin Trans. 2* **1975**, 1569.

(12) Fischer, E. *J. Mol. Struct.* **1982**, *84*, 219.

(13) Baraldi, I.; Momicchioli, F.; Ponterini, G. *Theochem.* **1984**, *110*, 187.

(14) Siegrist, A. E.; Liechti, P.; Meyer, H. R.; Weber, K. *Helv. Chim. Acta* **1969**, *52*, 2521.

(15) Gordon, A. J.; Ford, R. A. "The Chemist's Companion: A Handbook of Practical Data, Techniques and References"; Wiley Interscience: New York, 1972.

(16) Ghiggino, K. P.; Skilton, P. F.; Thistlethwaite, P. J. *J. Photochem.* **1985**, *31*, 111.

0002-7863/86/1508-1146$01.50/0

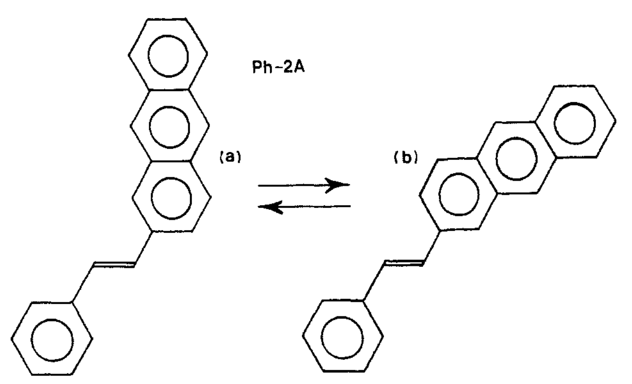

Figure 1. Proposed equilibrium for Ph-2A.

counting electronics incorporated Ortec modules, including a 454 timing filter amplifier, a 583 constant fraction discriminator, and a 457 time-to-pulse height converter as well as a Tracor Northern NS-710A multichannel analyzer. The data were transferred to a VAX computer for nonlinear least-squares iterative reconvolution analysis. Goodness of fit was assessed by inspection of residuals, autocorrelation function, and Durbin–Watson parameter as discussed previously.[16,17]

Time-resolved emission spectra could be recorded by using voltage discriminators on the output of the time-to-pulse height converter to select a "time window" in the decay profile. The monochromator was then synchronously scanned with the multichannel analyzer operating in the multichannel-scaling mode. These spectra were uncorrected for the wavelength response of the detection system.

Measurements below room temperature were conducted in an Oxford Instruments DN 704 liquid nitrogen cryostat, employing a DTC2 variable-temperature controller and fitted with nonbirefringent Suprasil-B windows. Cooling was at a rate of less than 3 K/min so as to eliminate the possibility of freezing the position of equilibrium by rapid thermal quenching.[5]

Results and Discussion

In an earlier study by Fischer and co-workers,[2,9] it was shown that for Ph-2A in toluene at 223 K the fluorescence emission spectrum could be described as a summation of two underlying component spectra, one having emission maxima at approximately 413, 436, and 462 nm and the other at 426, 452, and 482 nm. The contribution of each to the recorded luminescence varied with excitation wavelength, with the component at longer wavelengths being favored with excitation at the extreme red end of the observed absorption spectrum. This phenomenon was also observed in our laboratory in the steady-state emission spectra of Ph-2A at 25 °C, also suggesting the presence of two distinct absorption spectra; the variation in emission being attributable to different fractions of light absorbed by either rotamer. On the basis of the relative wavelength shift of the components, it should be possible to monitor the extreme blue edge of the emission and isolate only the fluorescence of one species, while observations at other wavelengths ought to contain contributions from both species. Figure 2 depicts two such fluorescence decay measurements of a series taken every 5 nm across the emission band. When monitored at 395 nm (Figure 2a), the decay of fluorescence is described excellently by a single-exponential function having a lifetime of about 28 ns. However, when monitored at lower energies (e.g., Figure 2b) the emission is only well described by a sum of two exponential decays. The fractional contribution of each decay component (f_i) to the steady-state emission intensity, as given by eq 2, varies with the wavelength of observation.

$$f_i = \frac{A_i\tau_i}{\sum_{j=1}^{n} A_j\tau_j} \qquad (2)$$

In this equation, τ_i is the lifetime of species i, A_i is its fitted preexponential factor (or intensity of each component at zero time), and n is the number of exponentials, here 2. In all instances, the two fitted lifetimes were invariant with the monitored wavelength, having values of 8.3 ± 1.1 and 28.25 ± 0.75 ns (3σ limits), and are comparable with recently determined values of ~9.3 and ~25.5 ns in benzene.[2]

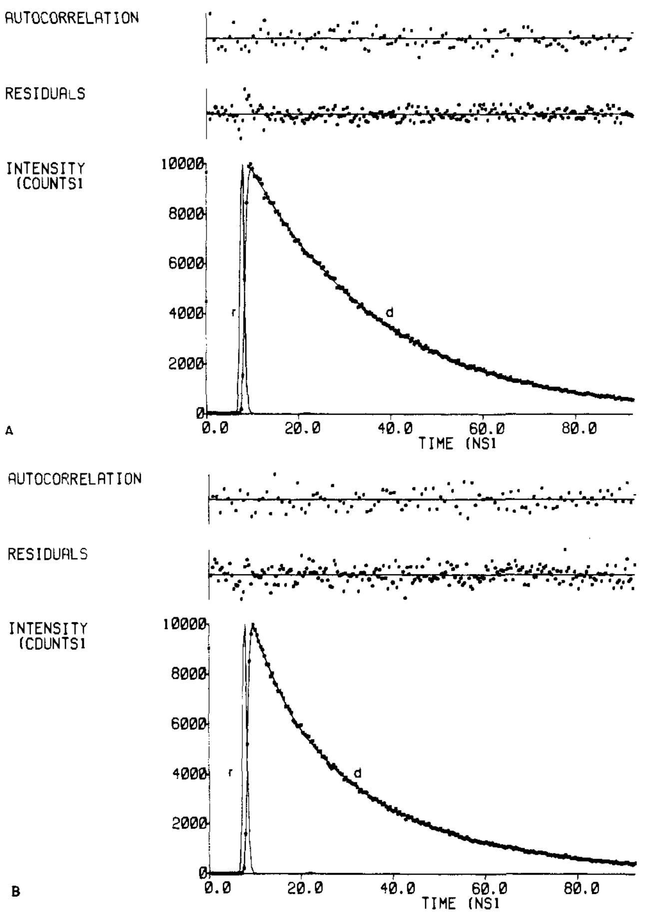

Figure 2. Experimental decay (d) and instrument response function (r) for Ph-2A in toluene at 25.0 °C fitted to $I(t) = \sum_{i=1}^{n} A_i e^{-t/\tau_i} + \mathrm{B}$, with A = preexponential factor (i.e., fluorescence intensity at zero time), τ = lifetime, and B = baseline parameter: (a) $n = 1$, $\lambda_{\mathrm{obsd}} = 395$ nm fitted curve with $\tau_1 = 28.39$ ns, $\chi^2 = 1.55$, and DW = 1.64; (b) $n = 2$, $\lambda_{\mathrm{obsd}} = 430$ nm fitted curve with $\tau_1 = 28.19$ ns, $\tau_2 = 8.11$ ns, $\chi^2 = 1.18$, and DW = 2.00. Excitation wavelength was 295 nm.

If a time-resolved emission spectrum is recorded immediately after excitation at 295 nm, it sould contain contributions from both species, whereas one recorded a considerable time after excitation should isolate a pure "long-τ" emission spectrum. The total emission spectrum, collecting photons arriving at the detector at all times following excitation, can also be measured. This is the equivalent of a steady-state emission spectrum. Early and late time-resolved emission spectra for Ph-2A are shown in Figure 3. Since it is known that at 395 nm the emission is homogeneous (i.e., the "long-τ" species) one can normalize the late-gated and early-gated spectra at this wavelength, giving, upon subtraction, the pure "short-τ" rotameric emission (also shown in Figure 3). Both spectra are structured but with the "short-τ" spectrum red-shifted relative to the "long-τ" spectrum. The two resolved components have maxima at 411, 434, and 458 nm and 420, 444, and 478 nm, which are in excellent agreement with both the earlier steady-state work of Fischer and recent measurements by Wismontski-Knittel et al.,[2] who used the method of phase resolution of spectra[18] to obtain the two component profiles having maxima at 409, 433, and 459 nm and 420, 447, and 476 nm. It should be noted here that the profiles could also be obtained by multiplying the fraction (f_i) of each component, as described by eq 2, by the measured total spectrum. This was indeed performed every 5 nm and exactly reproduced the resolved curves in Figure 3.

Since the time-resolved measurements clearly distinguished two separate lifetimes with no observable rise times, no appreciable

---

(17) Lampert, R. A.; Chewter, L. A.; Phillips, D.; O'Connor, D. V.; Roberts, A. J.; Meech, S. R. *Anal. Chem.* **1983**, *55*, 68.

(18) McGown, L. B.; Bright, F. V. Anal. Chem. **1984**, *56*, 1400A.

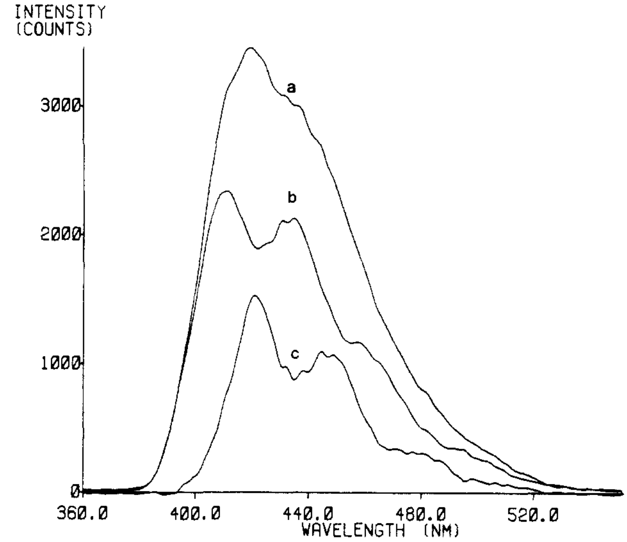

Figure 3. Time-resolved emission spectra for Ph-2A in toluene at 25.0 °C. Resolution was 0.8 nm/channel. Excitation wavelength was 295 nm: (a) early gated spectrum, gate width = 4.2 ns, delay = 2.1 ns; (b) late gated spectrum, gate width = 4.2 ns, delay = 60.1 ns, normalized to (a) at 395 nm (pure "long-τ" species); (c) difference spectrum (a) − (b) (pure "short-τ" species).

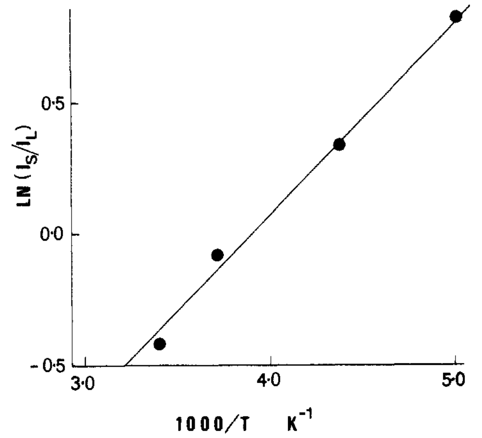

Figure 4. Van't Hoff plot for Ph-2A in toluene from steady-state fluorescence measurements. I_S and I_L are the emission intensities monitored at wavelengths where the "short-τ" rotamer and "long-τ" rotamer predominate (see text).

excited-state equilibration of the rotamers occurs under the conditions used here. Experiments in this laboratory have shown that the "long-τ" rotamer may principally be observed by monitoring the emission intensity (I_L) at 415 nm with an excitation wavelength of ~328 nm, while the "short-τ" rotamer may be followed by monitoring the emission intensity (I_S) at ~452 nm when exciting at 410 nm. Temperature variation of these signals over the range 200–294 K shows the "long-τ" rotamer signal decreases with an increase in temperature, while the signal from the "short-τ" rotamer shows a corresponding increase, providing evidence for a shift in equilibrium between the ground-state species with temperature. Figure 4 depicts a Van't Hoff plot using signals at these monitored wavelengths and indicates an apparent $\Delta H_{app} = 6.3 \pm 1.2$ kJ/mol (3 σ limit). This value will correspond not only to a shift in equilibrium but will also be influenced by variations in the nonradiative rates with temperature. From fluorescence lifetime measurements, the relative concentration of ground-state species can be estimated, since this ratio will be proportional to the ratio of the preexponential factors (A_i in eq 2) of the short- and long-τ components in the decay curves. The change in this ratio of preexponential factors as the temperature is varied can be used to construct a Van't Hoff plot that is not influenced by nonradiative rate changes. In Figure 5 the results of such an experiment are shown. The least-squares fit indicates a value of $\Delta H = 4.5 \pm 1.3$ kJ/mol (3 σ limit) for the difference in energy of the ground-state species, with the assumption that there are no significant changes in the relative radiative rates of the rotamers over the temperature range studied. From the Boltzmann distribution it is a simple matter to calculate $K_{eq}(298\ \mathrm{K}) = 0.163$ for the ground-state equilibrium constant between the rotamers. The energy difference between the ground-state levels of the rotamers (ΔH) is quite small, consistent with the significant population of each species at room temperature and with calculations for 1-phenyl-2-(2-naphthyl)ethylene.[13]

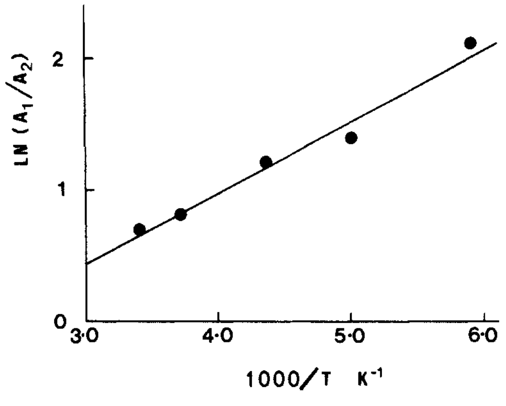

Figure 5. Van't Hoff plot for Ph-2A in toluene from fluorescence decay data. A_1 and A_2 are the preexponential factors of fitted dual exponential functions (see Figure 2) to the fluorescence decay measured at 430 and 500 nm as a function of temperature.

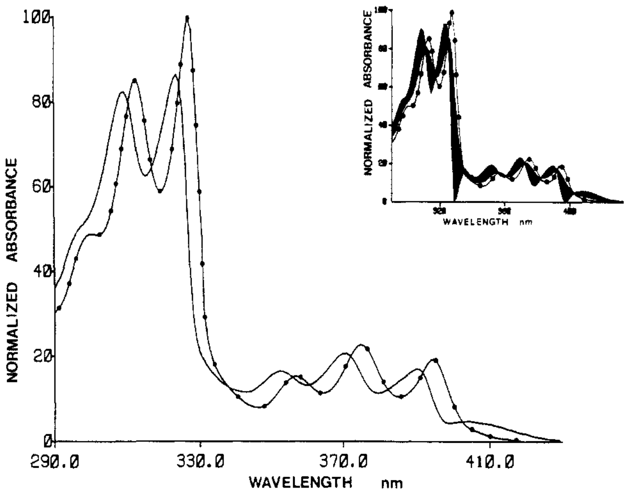

Figure 6. PCOMP-resolved rotameric absorption spectra, normalized by integrated absorption intensity: Solid line, "short-τ" species favored at higher temperatures; dotted line, "long-τ" species. Derived from spectra recorded in the temperature range 200–295 K. Inset: Full solution bands for resolved spectra.[25]

The mathematical least-squares method of principal component analysis (PCOMP)[3,19] is ideally suited to the case of Ph-2A. In this procedure, arbitrary spectra containing differing amounts of two underlying component spectra can be decomposed to reveal the two component spectra. No assumptions whatsoever are made as to curve profile. A unique solution is found provided one of the spectra does not fully overlap the other in its wavelength span.[19] Should this not occur, however, a narrow band of solutions is obtained where the midpoint of the band is taken as a reasonable estimate of the true solution. Absorption spectra were recorded over the range 200–295 K and digitized every 0.8 nm. A PCOMP analysis produced the resolved absorption spectra in Figure 6.[25] As can be seen, one has preferential absorption at the red extreme, identifying it as the short-τ absorption spectrum. Apart from this

---

(19) (a) Lawton, W. H.; Sylvestre, E. A. *Technometrics* **1971**, *13*, 617. (b) Warner, I. M.; Christian, G. D.; Davidson, E. R.; Callis, J. B. *Anal. Chem.* **1977**, *49*, 564. (c) Aartsma, T. J.; Gouterman, M.; Jochum, C.; Kwiram, A. L.; Pepich, B. V.; Williams, L. D. *J. Am. Chem. Soc.* **1982**, *104*, 6278.

long-wavelength feature, its structure is consistently blue-shifted and in a 1:1 correspondence with the long-τ vibrational features. Since the short-τ rotamer had the more red-shifted emission spectrum, it has the greater Stokes shift of the two species. Because the short-τ spectrum fully overlaps the long-τ absorption spectrum, solution bands had to be used. These had negligible width for the long-τ rotamer but were greater for the short-τ rotamer yet not wide enough to cause any vibrational feature to change significantly in relation to the long-τ spectrum. These spectra may be slightly distorted due to any minor shift of the individual spectra with a drop in temperature, though this should be minimal over the temperature range investigated.[20] Fluorescence excitation spectra were varied by viewing at different positions in the emission band, and a PCOMP analysis produced resolved excitation spectra essentially equivalent to the spectra in Figure 6.

Fluorescence quantum yields were obtained by using excitation at 295 and 410 nm. In the lattter case, slight interference to the emission by scattered excitation was subtracted off and the profile extrapolated. At 25 °C the calculated quantum yields were $\phi_{295} = 0.94$ and $\phi_{410} = 0.64$. Since the short-τ rotamer has its greatest absorbance relative to the long-τ rotamer at 410 nm and the quantum yield here is lower than at 295 nm, then the short-τ rotamer must have the smaller quantum yield (ϕ_S). This also has been noted previously in benzene solution.[2] It can readily be shown that, if the observed quantum yield is ϕ_{obsd} one rotamer will have $\phi > \phi_{obsd}$ while the other must have ϕ. From the 295-nm excitation measurement

$$0.94 < \phi_L < 1 \tag{3}$$

for the long-τ rotamer. The resolution of the total time-resolved emission spectrum into components can provide the relative contributions ρ_S and ρ_L of the short- and long-τ emissions to this spectrum. Equation 4 relates these fractions to individual absorbances and quantum yields of each species (A_S, ϕ_S and A_L, ϕ_L for the short- and long-τ species, respectively). In addition, the molar extinction coefficients ϵ can be calculated with

$$\rho_S = \left[\frac{1 - 10^{-A_S}}{1 - 10^{-(A_S+A_L)}}\right]\left[\frac{\phi_S}{\phi_{obsd}}\right] = \left[\frac{1 - 10^{-A_S}}{1 - 10^{-A_{obsd}}}\right]\left[\frac{\phi_S}{\phi_{obsd}}\right] \tag{4a}$$

$$\rho_L = \left[\frac{1 - 10^{-A_L}}{1 - 10^{-A_{obsd}}}\right]\left[\frac{\phi_L}{\phi_{obsd}}\right] \tag{4b}$$

$$A_S/A_L = (\epsilon_S/\epsilon_L)\ K_{eq} \tag{5}$$

where K_{eq} represents the ground-state equilibrium constant. Using eq 3 and 4b and the observed quantities $\rho_L = 0.901$, A_{obsd} (295 nm) = 0.672, and ϕ_{obsd} (295 nm) = 0.94 gives

$$0.477 < A_L < 0.536 \tag{6}$$

and from the measured absorbance at 295 nm

$$0.136 < A_S < 0.195 \tag{7}$$

From eq 4a and 7 and the aforementioned data

$$0.20 < \phi_S < 0.27 \tag{8}$$

where $\rho_S = 1 - \rho_L$ by definition.

Thus, one rotamer has $\phi_L = 0.97 \pm 0.03$ while the short-τ rotamer has $\phi_S = 0.24 \pm 0.04$, indicating that the respective radiative rates ($k_{rS} = \phi_S/\tau_S$ and $k_{rL} = \phi_L/\tau_L$) are $(2.9 \pm 0.7) \times 10^7$ s^{-1} and $(3.4 \pm 0.2) \times 10^7$ s^{-1} or equivalent within the accuracy of the experiment. This demonstrates that the fluorescence lifetimes differ by more than a factor of 3 due to the rotamers greatly differing in their nonradiative rates, which may be calculated as $k_{nrS} = 1/\tau_S - k_{rS} = 9.1 \times 10^7$ s^{-1} and $k_{nrL} = 1/\tau_L - k_{rL} = 1.4 \times 10^6$ s^{-1} for the short- and long-τ entities, respectively.

From eq 5–7 and K_{eq} it may also be concluded that

$$\epsilon_S \text{ (295 nm)} = (2.04 \pm 0.48)\epsilon_L \text{ (295 nm)} \tag{9}$$

Since the molar extinction coefficient for the long-τ species at 295 nm, ϵ_L (295 nm), was measured as $(3.48 \pm 0.25) \times 10^4$ M^{-1} cm^{-1} by cooling a known Ph-2A concentration to 200 K and reasonably assuming that the absorption spectrum is almost purely the long-τ rotamer at this temperature, the spectra in Figure 6 can be quantified if desired.

Conclusion

1-phenyl-2-(2-anthryl)ethylene has been characterized as existing in two rotameric forms in toluene solutions. The form having the shorter lifetime (8.3 ± 1.1 ns) and the smaller fluorescence quantum yield ($\phi_F = 0.24 \pm 0.04$) is characterized by having an emission spectrum to the red and an absorption spectrum mostly to the blue of the longer lifetime entity (28.25 ± 0.75 ns). This longer lifetime entity has $\phi_F = 0.97 \pm 0.03$ and the smaller molar extinction coefficient of the two. By analogy with the case of 1-phenyl-2-(2-naphthyl)ethylene[3,13] the most likely configurations for the long- and short-τ rotamers are the structures shown in Figure 1, parts a and b, respectively. Within experimental error, the two rotamers have equal radiative rates (3×10^7 s^{-1}), indicating that they differ in fluorescence lifetimes due to greatly differing efficiencies in their nonradiative deactivation pathways (k_{nr} (short-τ) = 9.1×10^7 s^{-1}, k_{nr} (long-τ) = 1.4×10^6 s^{-1}). Both trans–cis photoisomerization and intersystem crossing[21-24] are known to occur for the aryl ethylenes and differences in the efficiencies of these nonradiative processes for each rotamer may explain this result. In addition, the rotamers have been shown to be in a ground-state equilibrium with $\Delta H = 4.5 \pm 1.3$ kJ/mol with the shorter lifetime component favored at higher temperatures.

Supplementary Material Available: Plots of two eigenvectors and of coefficients from PCOMP analysis of rotamer absorption spectra for Ph-2A (2 pages). Ordering information is given on any current masthead page.

---

(20) Fischer, E. *J. Phys. Chem.* **1980**, *84*, 403.

(21) Lazare, S.; Bonneau, R.; Lapouyade, R. *J. Phys. Chem.* **1984**, *88*, 18.

(22) Krysanov, S. A.; Alfimov, M. V. *Chem. Phys. Lett.* **1983**, *98*, 176.

(23) Wismontski-Knittel, T.; Das, P. K. *J. Phys. Chem.* **1984**, *88*, 1168.

(24) Aloisi, G. G.; Mazzucato, U.; Birks, J. B.; Minuti, L. *J. Am. Chem. Soc.* **1977**, *99*, 6340.

(25) In the PCOMP analysis, 3 experimental spectra, recorded at 200, 249, and 295 K and each of 161 data points, were used. The two resolved components accounted for 99.92% of the variance of the original data.[19] The root-mean-square deviation of the calculated composite curves from the original data was better than 1% of the maximum absorbance. Plots of the two eigenvectors and coefficients[19c] are available as supplementary material.